Phase transitions in the Ising square lattice with next-nearest-neighbor interactions

D. P. Landau
Department of Physics and Astronomy, University of Georgia, Athens, Georgia 30602
(Received 12 April 1979)

An importance sampling Monte Carlo method has been used to study $L \times L$ Ising square lattices with periodic boundary conditions. The behavior of the thermal and magnetic properties was determined over a wide range of R, the ratio of next-nearest- to nearest-neighbor coupling. From these data we have extracted the R dependence of the critical temperature and a range of other critical parameters. Within our experimental error the critical exponents are independent of R but the critical amplitudes are not. The data do however suggest a change in α for R slightly greater than $\frac{1}{2}$. Variations in critical entropy and internal energy may be as large as those resulting from changes in lattice or spin dimensionalities. Our results are compared and contrasted with those obtained by a range of theoretical methods.

I. INTRODUCTION

The Ising square lattice with nearest-neighbor (nn) coupling is an exactly soluble model[1] which has served as a cornerstone for modern critical-point theory and as a testing ground for many approximate theoretical approaches. In a previous paper[2] we used a Monte Carlo technique to study the finite-size behavior of this model and showed that the data, when properly interpreted, could be used to obtain accurate values of the bulk properties and ordering temperature of the infinite lattice. With the addition of an applied magnetic field or next-nearest-neighbor (nnn) coupling the model is no longer exactly soluble by presently available theoretical techniques. Different approximate methods have been used to attack the extended model but the differences in the results suggest alternative results are needed to check them. In this paper we shall apply the Monte Carlo method to the zero-field nnn model:

$$\mathcal{H} = K_{\mathrm{nn}} \sum_{\substack{\mathrm{nn} \\ \mathrm{pairs}}} \sigma_i \sigma_j + K_{\mathrm{nnn}} \sum_{\substack{\mathrm{nnn} \\ \mathrm{pairs}}} \sigma_i \sigma_k \ , \tag{1}$$

where $\sigma_i, \sigma_j, \sigma_k = \pm 1$ and the ratio between nnn and nn coupling will be written $R = K_{\mathrm{nnn}}/K_{\mathrm{nn}}$. Naive application of universality concepts[3] would predict that the addition of nnn coupling should not affect the critical exponents. The situation may well be more complicated, however, since several "similar" models with short-range interactions[4–6] have been shown to possess "anomalous" exponents due to a special ground-state degeneracy. The behavior of this model is of interest, not only because of the existing theoretical questions, but also because recent experimental work[7,8] has shown that real pseudo-two-dimensional systems exist and the model may thus have physical significance. In addition, when other, more conclusive experimental evidence is unavailable, the critical energy or critical entropy is sometimes used[9] to predict the nature of the Hamiltonian appropriate to the physical system being studied. It is known[9] that these parameters are strongly dependent on spin and lattice dimensionalities but the dependence on competing, short-range interactions has not been determined over a wide range of R.

The ground-state properties of this model can be calculated exactly and the possible ordered states are shown in Fig. 1. The bulk properties are independent

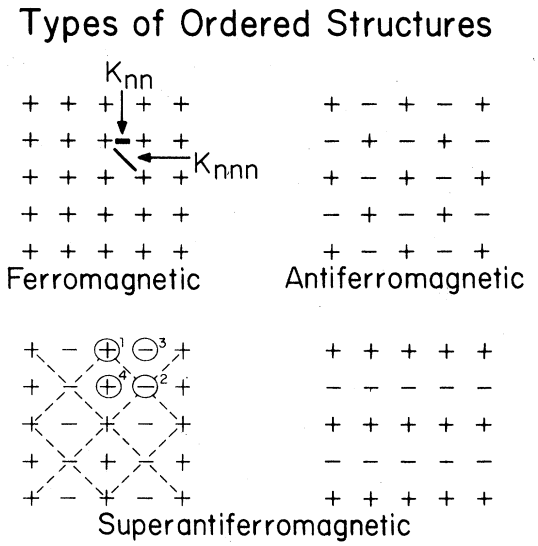

FIG. 1. Possible ground states which can occur for the Ising square lattice with nearest- and next-nearest-neighbor coupling. The four sublattices comprising the superantiferromagnetic ground state are made of sites displaced by multiples of two lattice spacings from the sites labeled 1–4. The dashed lines form one pair of antiferromagnetically coupled sublattices.

of the sign of K_{nn} as long as appropriate definitions are used, e.g., the staggered magnetization of the antiferromagnet is equivalent to the spontaneous magnetization of the corresponding ferromagnet. For convenience we shall restrict ourselves to the case of antiferromagnetic nn interactions ($K_{nn} > 0$) but the results are of course relevant to the ferromagnetic case $K_{nn} < 0$. For $R > 0.5$ the system breaks up into two *pairs* of interpenetrating antiferromagnetic systems. The resultant structure is doubly degenerate (see Fig. 1) and is given the name "superantiferromagnetic" (SAF). (In the limiting cases $R \to \pm\infty$ the lattice breaks up into two uncoupled, interpenetrating antiferromagnetic square lattices composed of nnn bonds. Therefore the limiting value $kT_c/|K_{nnn}|$ is known exactly.)

Several theoretical methods have been applied to the nnn-Ising square lattice [Eq. (1)], but the temperature variation of the thermodynamic properties for a wide range of R is not really well known. Bitterlich and Jellito[10] used a matrix method to find exact solutions for small $L \times L$ square lattices ($L \leq 8$) with periodic boundary conditions. The results are of limited value since exact solutions[11] for finite $L \times L$ square lattices with $R = 0$ indicate that an $L = 8$ lattice is much too small to allow a reliable extrapolation to $L = \infty$. The model has also been recast into the formalism used for many fermion theory[12–14] but the partition function could still only be solved approximately by a variety of perturbational methods. The greatest progress has been made using series expansions[15–17] and renormalization-group methods.[18,19] Dalton and Wood[15] have derived series expansions appropriate for Eq. (1) and have analyzed them in detail for $0 \geq R \geq -1$. For $R > 0$ the series became erratic; Dalton and Wood were unable to analyze them although Takase[16] was able to analyze the low-temperature series for small positive R. However, on the basis of an analysis of the low-temperature series expansions Wu[17] inferred that the low-temperature exponents are in general non-Ising-like for $R \neq 0$. (Fisher and Camp[20] earlier showed that the $R = 0$ model is unique in that the spin-spin correlation function has a non-Ornstein-Zernike decay below T_c.) A renormalization-group investigation was carried out in a four-cell cluster approximation[18] and the critical temperature was computed for $-1 \leq R \leq +1$. Nightingale,[21] however, introduced a transformation relating the properties of the model to a finite system with modified interactions and predicted nonuniversal behavior for $R > 0.5$. Other theoretical approaches have also predicted[22] nonuniversal behavior for $R > \frac{1}{2}$. Preliminary results of our Monte Carlo studies have been presented elsewhere[23] and more recent results[16,24] are available for smaller lattices.

The goal of this work has been to determine the dependence of the thermodynamic properties over the widest possible range of R. Greater precision for each data point could have been achieved but only at the expense of the range of interactions which could have been treated. In Sec. II we shall briefly describe the Monte Carlo method and introduce the scaling theories needed for the interpretation of the data. Section III contains extensive data for the thermal and magnetic behavior, and in Sec. IV we shall analyze these data in order to study the critical behavior and extract a number of characteristic cooperative parameters. In Sec. V we shall summarize and conclude.

II. METHODS OF STUDY

A. Monte Carlo technique

We have used an importance sampling Monte Carlo method to study $L \times L$ lattices with periodic boundary conditions applied to eliminate surface effects. (Only even values of L were used so that no "misfit seams" were present.) Successive states were generated using a single-site spin-flip mechanism where the transition probability was

$$W(\sigma_i \to -\sigma_i) = W_0 \exp(-\Delta E/kT) \quad , \tag{2}$$

where ΔE was the energy difference [calculated from Eq. (1)] involved in the transition. Thermodynamic averages for the order parameter, internal energy, and spin-spin correlation functions were then determined by calculating the weighted statistical mechanical average over the limited number of configurations sampled. (For $R < 0.5$ the order parameter was taken to be the absolute value of the staggered magnetization. For $R > 0.5$ the order parameter was instead computed from the average of the absolute values of the four sublattices.) Thermodynamic response functions, e.g., specific heat C, ordering (staggered) susceptibility χ^+, and nonordering susceptibility χ were computed from the fluctuations. The technique has been described in detail elsewhere[25] and the details of our computational algorithm have been given in Ref. 2.

Data were accumulated over the range $-100 \leq R \leq +3$ (the reason for the large negative value will become clear in Sec. IV). The range of R should be sufficiently broad to answer theoretical questions concerning the critical behavior and to provide results for comparison with data obtained on physical "two-dimensional Ising" systems. Since we were primarily interested in the infinite lattice behavior of the model, we have only studied systems with $L \geq 10$. The inclusion of nnn coupling increased the computing time needed by almost 30% over the $R = 0$ case and the number of states sampled is correspondingly smaller. Nonetheless, at least 600 MCS (Monte Carlo steps per spin) were taken for each data point near T_c and in some cases as many as 2000 MCS were used. The results shown in Sec. III represented the

average value obtained from anywhere from two to five repetitions of the same point using different initial conditions and random numbers. The maximum lattice size studied was $L=60$.

B. Finite-size scaling theory

The properties of finite simple Ising lattices are known to be strongly size dependent near the critical temperature. A finite-size scaling theory has been developed by Fisher[29] to describe these effects in terms of infinite lattice critical exponents. According to this finite-size scaling theory, the free energy of an $L \times L$ lattice is given by the scaling ansatz:

$$F(L,T) = L^{-\Psi} \mathfrak{F}^0(L^{1/\nu} t) \ , \tag{3}$$

where $\Psi = (2-\alpha)/\nu$, $t = |1 - T/T_c(\infty)|$ with $T_c(\infty)$ being the infinite-lattice transition temperature, and $\mathfrak{F}^0$ is a scaling function involving the scaled variable $x = L^{1/\nu} t$. The shift of the "pseudo-ordering" temperature $T_c(L)$ (usually defined by the location of the specific-heat peak) is given by

$$\delta T_c = [1 - T_c(L)/T_c(\infty)] = aL^{-1/\nu} \ . \tag{4}$$

The finite-size scaling of the free energy leads to scaling relations for the bulk properties. For example, for the order parameter m of a system with periodic boundary conditions

$$mL^{\beta/\nu} = f(x) \underset{x\to\infty}{\to} Bx^{\beta} \ . \tag{5}$$

This approach has proven quite successful in treating Ising models[2,30] although the ultimate reliability of the analysis obviously depends on the accuracy of the finite lattice data.

C. Crossover scaling theory

The possibility of scaling with respect to the interaction parameter for a system with competing interactions has been studied for a system with isotropic interactions[31] and should be appropriate for an Ising model as well. Here we might consider four limiting cases $R \to \infty$, $R \to -\infty$, and $R \to \frac{1}{2}$ from above and below. The scaling parameter Δ would be different in each case, e.g., $\Delta = R^{-1}$ for $R \to \infty$ and $\Delta = R - \frac{1}{2}$ from above. According to the standard treatments of crossover scaling theory[31–35] we can write the asympotic variation of the critical temperature as

$$T_c(\Delta) - T_c(\Delta=0) \propto \Delta^{1/\phi} \ , \tag{6}$$

where ϕ is the characteristic "crossover exponent." Following Chang *et al.*[31] we write the free energy

$$F(h,t,\Delta) = t^{2-\alpha} F(t^{\Psi} h, t^{-\phi}\Delta) \ , \tag{7}$$

where $t = |1 - T/T_c(\Delta)|$, h is an applied magnetic field, and the exponent $\Psi = \frac{1}{2}(2-\alpha+\phi)$. From Eq. (7) expressions for the zero-field critical behavior of the bulk properties may be readily derived, e.g.,

$$m = t^{2-\alpha-\Psi} f(t^{-\phi}\Delta) \ , \tag{8a}$$

$$\chi^+ = t^{2-\alpha-\Psi} g(t^{-\phi}\Delta) \ , \tag{8b}$$

$$C = t^{-\alpha} h(t^{-\phi}\Delta) \ . \tag{8c}$$

In the limiting case of $R \to -\infty$ ($\Delta = -R^{-1} \to 0$), these expressions must eventually reproduce simple Ising critical behavior. An analysis of Eq. (8) then indicates that $\phi = \gamma = 1.75$. In general for $\Delta \neq 0$ the critical behavior is given by

$$m = B(\Delta) t^{\beta'} \ , \tag{9a}$$

$$\chi^+ = C(\Delta) t^{-\gamma'} \ , \tag{9b}$$

$$C = A(\Delta) t^{-\alpha'} \ , \tag{9c}$$

where α', β', and γ' are the new critical exponents and the amplitudes are given by

$$B(\Delta) = B_0 \Delta^{(2-\alpha-2\beta'-\phi)/2\phi} \ , \tag{10a}$$

$$C(\Delta) = C_0 \Delta^{(\phi-\gamma')/\phi} \ , \tag{10b}$$

$$A(\Delta) = A_0 \ . \tag{10c}$$

For $R < \frac{1}{2}$ we certainly expect that the critical exponents retain their Ising values and the amplitudes are thus constant as $R \to -\infty$. Since it is possible that new exponents (continuously variable[21,22]) appear for $R > \frac{1}{2}$ the variation of the amplitudes may be more complicated.

An alternative formalism[35] for the crossover scaling analysis would be one in which the correlation length diverges exponentially instead of according to a power law

$$\xi = \bar{\xi} \exp(ct^{-\bar{\nu}}) \ . \tag{11}$$

The variation of $T_c(\Delta)$ may then take on a different form, e.g.,

$$T_c(\Delta) - T_c(\Delta=0) \propto [\ln(\xi_0 \Delta^{1/\bar{\phi}})^{-1}]^{1/\bar{\nu}} \ , \tag{12}$$

where $\bar{\phi}$, $\bar{\nu}$, etc., are new exponents. The amplitude predictions then become

$$A(\Delta) = A_0 \Delta^{\bar{\alpha}/\bar{\phi}} \ , \tag{13a}$$

$$B(\Delta) = B_0 \Delta^{\bar{\beta}/\bar{\phi}} \ , \tag{13b}$$

$$C(\Delta) = C_0 \Delta^{\bar{\gamma}/\bar{\phi}} \ . \tag{13c}$$

III. RESULTS

A. Thermal properties

The data obtained showed qualitatively similar behavior to those observed for the nn only model. In

fact, the only significant difference was the appearance of a metastability which occurred at low temperatures for R near 0.5. In this case the SAF and AF (antiferromagnetic) states are quite close together in energy and the system can be "trapped" at very low temperature in a state which is not really much higher in energy than the ground state. An example of this metastable behavior is shown in Fig. 2 where the internal energy data are plotted for an $L=40$ system with $R=0.7$ in an initial AF state. As the data showed, the system persisted in the metastable AF state as the temperature was varied until $kT/K_{nn}=1.18$. It is in fact possible to draw a single curve through the data shown with a maximum deviation of just over 1%. Any data showing evidence of metastable behavior were discarded from the analysis.

The finite-size dependence of the thermal properties was quite similar to that observed earlier[2] for $R=0$. The internal energy showed very little effect of finite size outside of a narrow region near T_c. Within this region infinite lattice results were obtained using an extrapolation in L^{-1}. Because of the similarity to the previously published $R=0$ results, data for various lattice sizes will not be presented here. The specific-heat peak was rounded and shifted to higher temperature as the lattice size decreased. The infinite lattice critical temperatures $T_c(R)$ were determined using a linear extrapolation with L, i.e., Eq. (4) with $\nu=1$. If the critical behavior is non-Ising-like, ν may take on a different value; however, the lattices studied here are sufficiently large that we

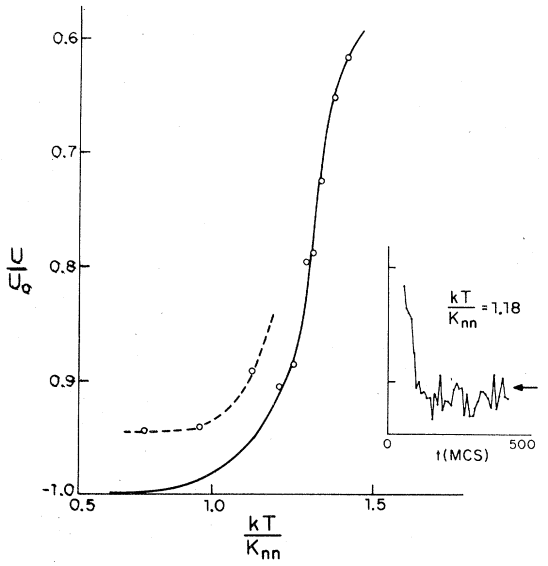

FIG. 2. Metastable AF state for $R=0.7$. System was initialized in the AF state. The inset shows the time dependence of the internal energy U at $kT/K_{nn}=1.18$ as the system drops to the SAF state. The arrow shows the mean value over the entire time interval shown. (U_0 is the internal energy at $T=0$).

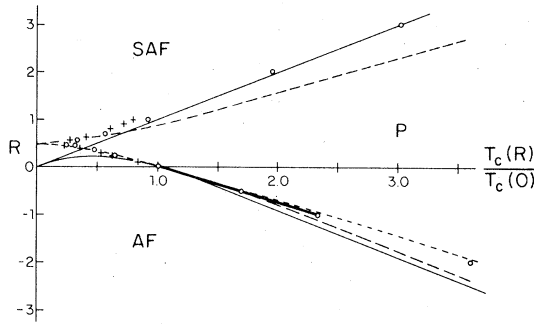

FIG. 3. Variation of the critical temperature with nnn coupling. The open circles are the Monte Carlo values. Theoretical estimates for $T_c(R)$ are: —— series expansions by Dalton and Wood (Ref. 15); ———— Gibberd (Ref. 13); —— Kawakami and Osawa (Ref. 12); – – – Fan and Wu (Ref. 14); + renormalization-group theory (Ref. 18).

estimate the additional error in extrapolation to $L=\infty$ to be no more than $\frac{1}{2}\%$ due to uncertainty in ν. (The R dependence of T_c will be discussed in some detail in Sec. IV.) The variation of $T_c(R)$ is depicted in Fig. 3 and the normalized internal energy results are then plotted versus $T/T_c(R)$ in Fig. 4.

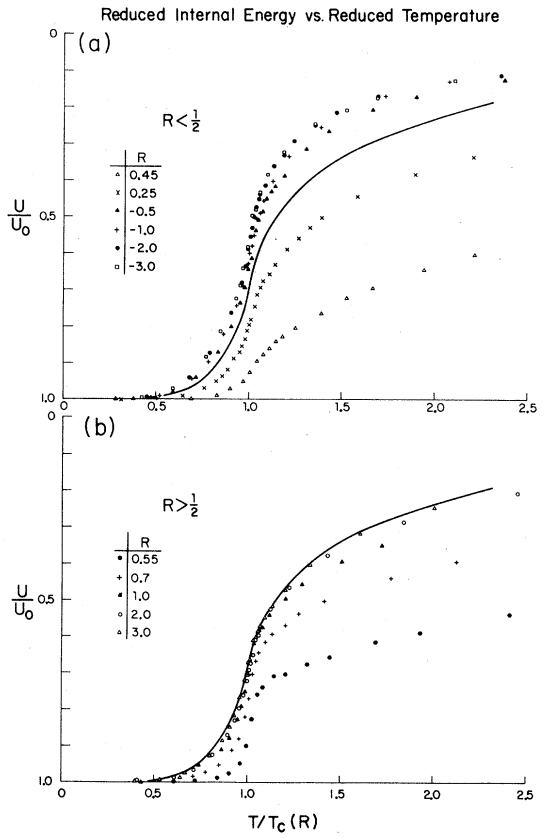

FIG. 4. Temperature dependence of the internal energy. The data points are normalized by the internal energy at absolute zero U_0. The solid curves give the variation for $R=0$.

(Because of the widely different values of R included in this study, the temperature range of interest, measured in units of K_{nn}/k, varies significantly from one value of R to another.) Even when plotted in this reduced form, the internal energy data show significant dependence on R. For $R > \frac{1}{2}$ the internal energy values quickly approach the nn only curve as R increases and by the time $R = 3$ the two curves are almost indistinguishable. For $R < \frac{1}{2}$, however, the data show a much wider variation lying below the nn only curve for $R > 0$ and then crossing over to lie above the curve for $R < 0$. The data for $R < 0$ begin to approach the $R = 0$ curve again only when much more strongly negative values of R than those shown in Fig. 4 are reached.

The specific-heat results also vary significantly with R. Data for several different R values are compared in Fig. 5. For $R < 0$ the specific heat is no longer symmetric about T_c but is reduced at high temperature and increased at low temperature with respect to the nn only curve. For $\frac{1}{2} > R > 0$ the reverse is true. The specific heat behaves yet differently for $R > \frac{1}{2}$ but quickly approaches the nn only curve as R increases.

The case $R = \frac{1}{2}$ is special in that, as shown in Fig. 3, there is no transition at any finite temperature. The specific heat for $R = \frac{1}{2}$ behaves quite differently than for other R values and it shows no sharp peak. The results, shown in Fig. 6, indicate only a low rounded maximum.

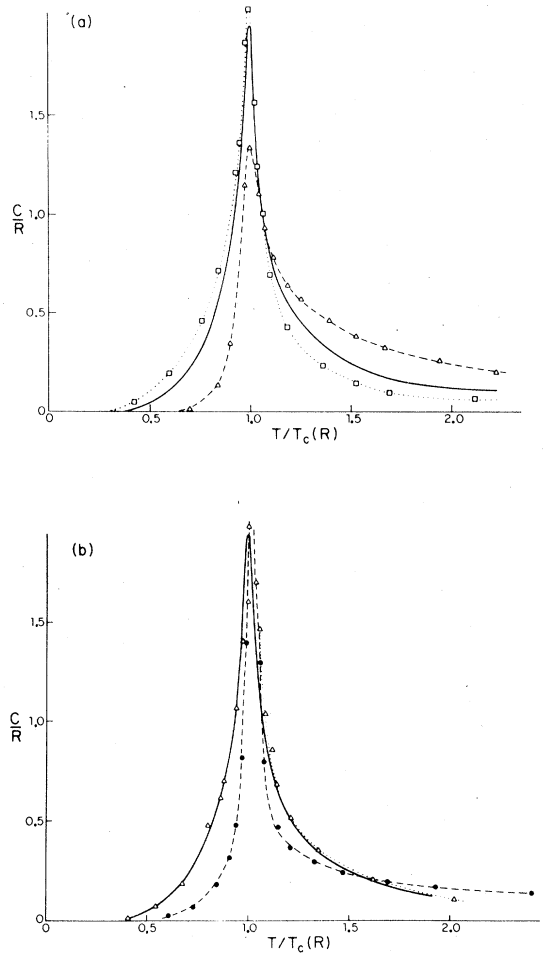

FIG. 5. Specific heat vs temperature. (a) Results for $R < 0.5$: solid line, $R = 0$; dotted line with open squares, $R = -3.0$; dashed line with open triangles, $R = +0.45$. (b) Results for $R > 0.5$ dashed line with full circles, $R = +0.55$, dotted line with open triangles, $R = 2.0$. The behavior for $R = 0$ is shown for comparison, solid line.

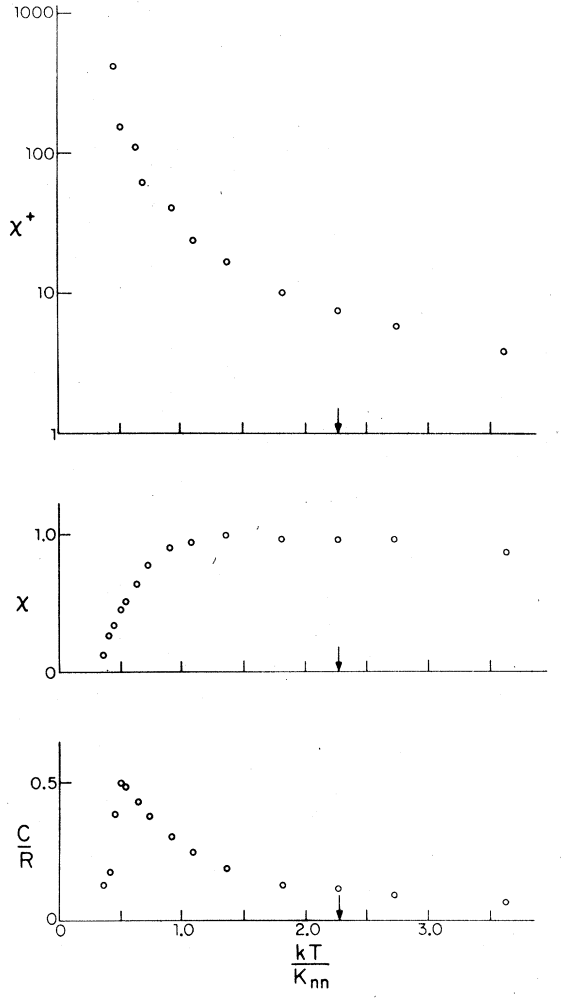

FIG. 6. Temperature dependence of the bulk properties for $R = \frac{1}{2}$: (a) staggered susceptibility; (b) (nonordering) susceptibility; and (c) specific heat. The arrows show the location of $T_c(0)$ for comparison.

B. Magnetic properties

The temperature dependence of the order parameter was qualitatively the same for all values of $R \neq 0$ as for $R = 0$. The low-temperature results showed very little finite-size effects. Very close to $T_c(R)$ finite-size rounding began to play a role and at a high temperature a residual lattice size dependent "tail" remained. This "tail" did of course extrapolate to zero as $L \to \infty$. In Fig. 7 we show the resultant estimates for the infinite lattice behavior for various values of R. These results show that for R near to $\frac{1}{2}$ the order parameter stays quite close to 1.0 until very close to $T_c(R)$. Here too as R is reduced below zero the order-parameter data fall below the $R = 0$ curve and approach it only for much more negative values of R than those plotted here. In contrast, as R increases from $\frac{1}{2}$, the data very quickly approach the $R = 0$ curve.

The behavior of the magnetic susceptibility is shown in Fig. 8. Again the qualitative behavior is the same for $R \neq 0$ as for $R = 0$. Within experimental error the maximum slope in χT vs T occurs at $T_c(R)$ with a maximum in χT occurring at much higher temperature. There are, however, marked differences in the values of the critical susceptibility χ_c and the location and magnitude of the susceptibility maximum. The susceptibility data for $R = \frac{1}{2}$ (see Fig. 6) also show a very broad maximum.

Typical results for the staggered susceptibility are shown in Fig. 9 for $R < \frac{1}{2}$. (Due to the way the order parameter was defined and the computer program was written, χ^+ was only determined for $R \leq \frac{1}{2}$.) The data show a dramatic peak in χ^+; for $R > 0$ the staggered susceptibility lies above the $R = 0$ curve, but for $R = -3.0$ the reverse is true. For $R = \frac{1}{2}$ the

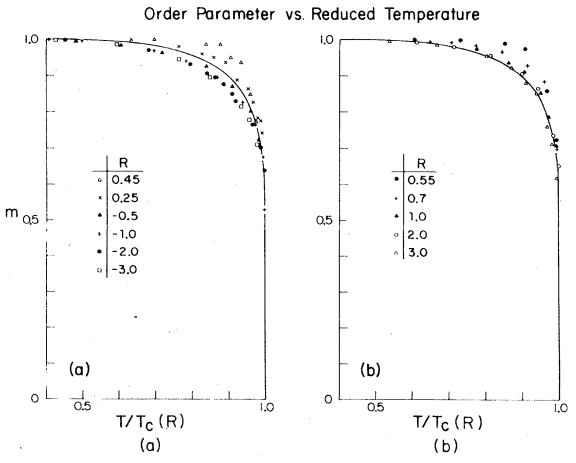

FIG. 7. Order parameter vs temperature. The solid line shows the variation for $R = 0$.

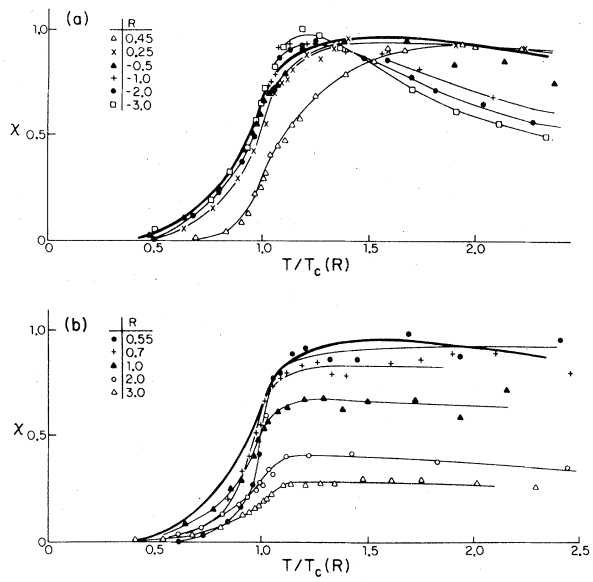

FIG. 8. (a),(b) Temperature dependence of the magnetic ("nonordering") susceptibility. The heavy solid curve shows the variation for $R = 0$.

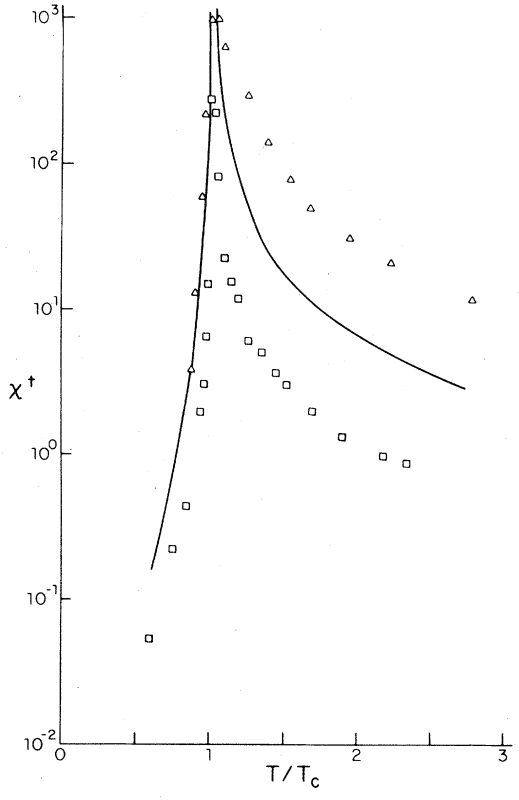

FIG. 9. Temperature dependence of the staggered ("ordering") susceptibility: □, $R = -3.0$; Δ, $R = +0.45$. The solid curve represents the $R = 0$ behavior.

susceptibility rises continuously all the way down to the lowest temperature studied (see Fig. 6).

C. Spin-spin correlations

The spin-spin row correlations $\Gamma(r)$ were computed out to $r=10$, and we show the temperature dependence of the first few r values for $R=+0.45$ and -2.0 in Fig. 10. The data indicate that the correlations fall off monotonically for all values of r and also that the decay with increasing temperature is much more rapid for $R=-2.0$ than for $R=+0.45$. For $R>\frac{1}{2}$ the row correlations are zero for odd r. Since the SAF structure is composed of two interpenetrating antiferromagnets, the crystallographic nnn correlation plays the role of the nn correlation for $R<\frac{1}{2}$ and the crystallographic diagonal correlations play the role of the row correlations. The first three "row" correlations for $R=+2.0$ are also shown in Fig. 10; the data points lie very close to the equivalent $R=0$ values. The correlation functions are clearly strongly dependent on R, particularly above the ordering temperature.

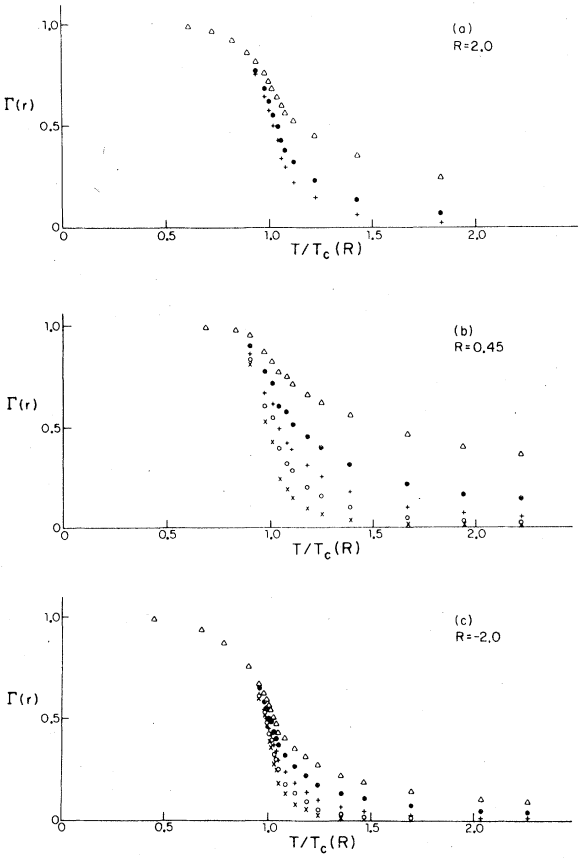

FIG. 10. Temperature variation of near-neighbor row spin-spin correlations: (a) diagonal correlations for $R=+2.0$: $r=\sqrt{2}$, Δ; $r=2\sqrt{2}$, $\bullet$; $r=3\sqrt{2}$, $+$; (b) results for $R=+0.45$; and (c) results for $R=-2.0$. Data are for: $r=1$, Δ; $r=2$, $\bullet$; $r=3$, $+$; $r=4$, $\circ$; and $r=6$, $\times$.

IV. ANALYSIS AND DISCUSSION

A. Variation of $T_c(R)$

The results for the dependence of T_c on R can be analyzed using the crossover scaling theory presented in Sec. II. By considering the variation of T_c with R when $K_{\rm nnn}$ is held fixed and $K_{\rm nn}$ is allowed to change, we can study the crossover behavior in the limits $R\rightarrow\pm\infty$. In this case the scaling parameter $\Delta=|R^{-1}|$ and Eq. (6) can most usefully be rewritten

$$\frac{k[T_c(\infty)-T_c(R)]}{K_{\rm nnn}}=x_0R^{-1/\phi}\ . \tag{14}$$

Since the system separates into two interpenetrating nnn lattices, the asymptotic critical temperature $kT_c(\infty)/K_{\rm nnn}$ is identical to the ordinary nn square lattice value $kT_c(0)/K_{\rm nn}$. In Fig. 11 a log-log plot shows the variation of $[T_c(\infty)-T_c(R)]$ for both $R\rightarrow-\infty$ and $R\rightarrow+\infty$. For $R\rightarrow+\infty$, $T_c(R)$ *very* quickly approaches $T_c(\infty)$ and by the time $R=+3$, the difference is essentially negligible. Although there is no clearly linear region in the plot, it is possible to draw a straight line through the large R values with slope ~-0.21 corresponding to $\phi\sim0.48$. For $R\rightarrow-\infty$ the results behave quite differently and smoothly approach a straight line with slope $=0.57$, corresponding to $\phi=\gamma=1.75$, as predicted,[31,34] and are well described by the asymptotic form for $|R^{-1}|\lesssim0.1$. Since the results for much less negative values of R yielded rather large differences

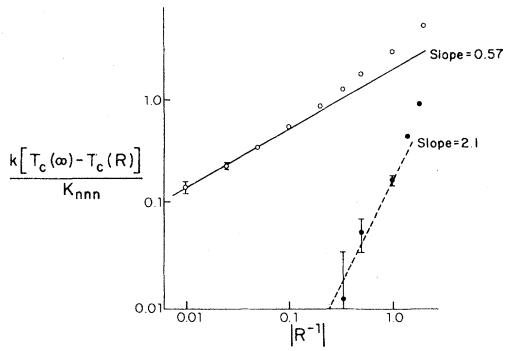

FIG. 11. Dependence of T_c on R as $R\rightarrow\infty$. The open circles are the Monte Carlo estimates for $R<\frac{1}{2}$ and the straight-line best fit to the large $|R|$ data for $R<0$ is constrained to have slope $=\gamma^{-1}=0.57$. Closed circles are estimates for $R>\frac{1}{2}$.

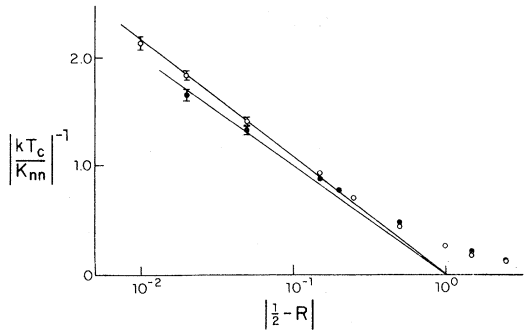

FIG. 12. Variation of $T_c(R)$ as $R \to \infty$. Results are for: $R < \frac{1}{2}$, ○; $R > \frac{1}{2}$, ●. Solid lines are the best fits to the asymptotic form given by Eq. (12).

$k[T_c(\infty) - T_c(R)]/K_{nnn}$ yet were not consistent with Eq. (14), we continued the calculations all the way to $R = -100$ in order to more carefully examine the asymptotic crossover behavior. The difference in results for $R \to +\infty$ and $R \to -\infty$ suggests that either the critical exponents for $R \to +\infty$ are non-Ising-like or that the asymptotic behavior occurs so close to $kT_c(\infty)/K_{nnn}$ that we cannot resolve it.

The same analysis can be applied to the results for $R \to \frac{1}{2}$ from above or below. Plots similar to Fig. 11 were made but taking $\Delta = |\frac{1}{2} - R|$ instead of $\Delta = R^{-1}$. The data were nowhere consistent with Eq. (6) so we decided to test for the alternative form given by Eq. (12) by making a semilogarithmic plot instead. An analysis of the behavior for $R = \frac{1}{2}$ (to be presented shortly) suggests that $\bar{\nu} \approx 1$; hence, we shall use $\bar{\nu} = 1$ in the following. In Fig. 12 we see that the variation of T_c is quite consistent with this crossover form for $R \to \frac{1}{2}$ from below. The results for $R > \frac{1}{2}$ appear to approach an asymptotic logarithmic form (with a modified amplitude) but only for the smallest values of $|R - \frac{1}{2}|$ studied. (We also cannot exclude the possibility, however, that asymptotic form never becomes logarithmic for $R > \frac{1}{2}$.)

B. Short-range order

1. $R \neq \frac{1}{2}$

We have already seen that transitions occur for all $R \neq \frac{1}{2}$ and are therefore interested in the behavior above $T_c(R)$. The data shown in Sec. IV A clearly indicate that the behavior of the thermal and magnetic properties above T_c are quantitatively different. One very useful way of studying these differences is to compare the temperature dependence of the internal energy and the nn spin-spin correlation function $\Gamma(r=1) = \langle \sigma_i \sigma_j \rangle_{nn}$. (For $R = 0$ the two are identical at all temperatures.) In Fig. 13(a) we show the ratio of the two properties for $R < \frac{1}{2}$. Figure 13(b) shows an equivalent plot for $R > \frac{1}{2}$ but with $\Gamma(r=1) = \langle \sigma_i \sigma_j \rangle_{nn}$ replaced by $\langle \sigma_i \sigma_j \rangle_{nnn}$ because of the interpenetrating lattices which occur for these R values. In both cases the ratio is very close to 1 up to $\sim 0.95 T_c$. Above T_c the ratios quickly deviate from one another indicating the difference in the distribution of energy in the short-range order as suggested by the spin-spin correlation data in Fig. 10.

Previous studies by Stephenson[36] have indicated that for $0 < R < \frac{1}{2}$ the spin-spin correlation functions should show a nonisotropic oscillatory behavior above a characteristic "disorder temperature" T_d. This effect becomes observable, for example, when the nnn correlation function changes sign as the temperature increases. Very high-temperature data for $R = +0.25$ and $+0.45$ shown in Fig. 14 show clear evidence of a disorder point, whereas similar data for $R = -2.0$ show no such effect.

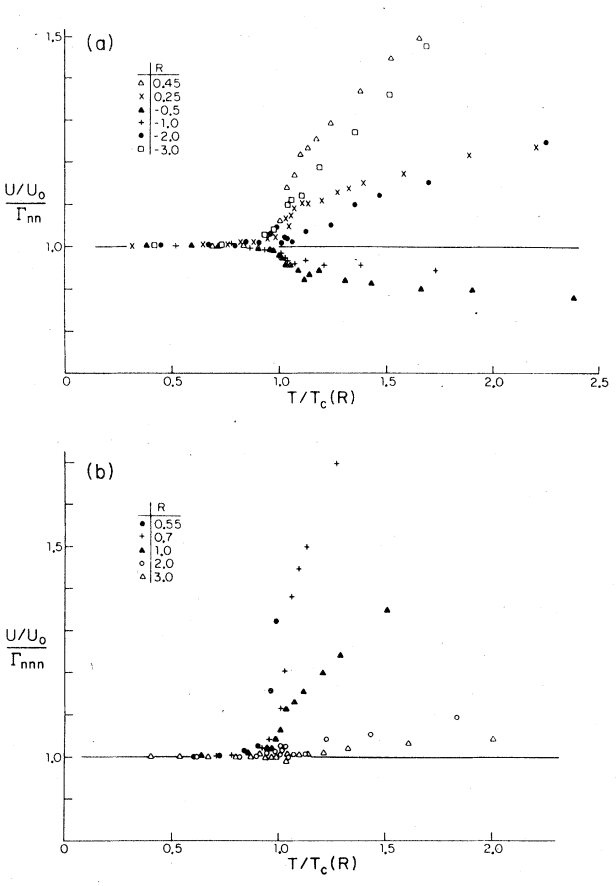

FIG. 13. (a),(b) Temperature dependence of the ratio of the internal energy to nn spin-spin correlation function. The straight line with constant value 1 shows the result for $R = 0$.

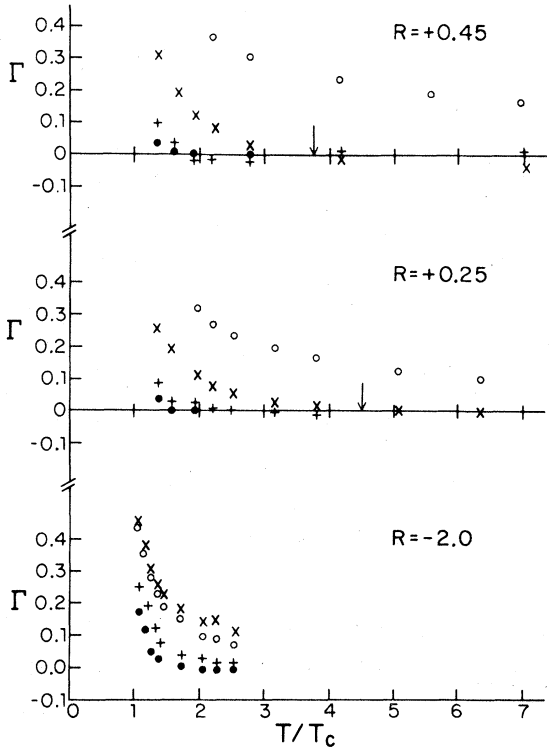

FIG. 14. Comparison of nn and nnn spin-spin correlation functions. The arrows indicate the approximate temperature at which the nnn correlation changes sign. The open circles show the nn correlations, and the ×'s show the nnn correlations. The second and third diagonal correlations are given by + and ○, respectively.

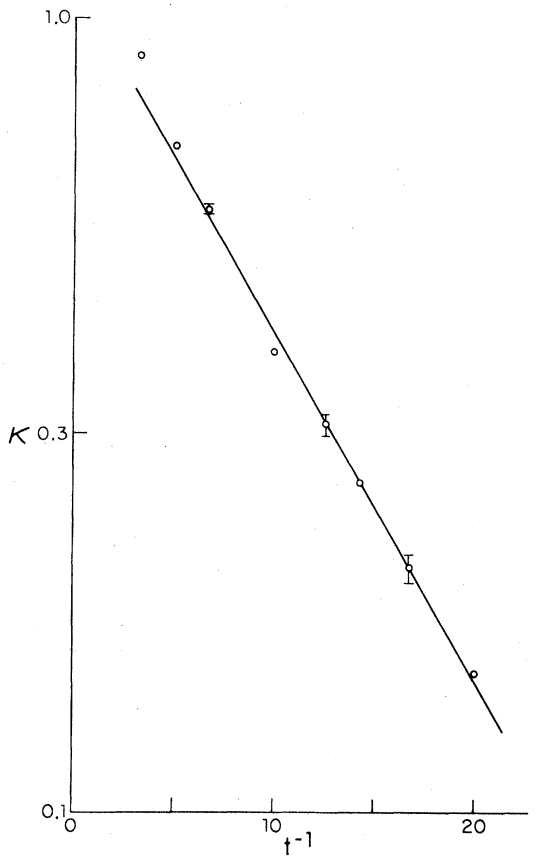

FIG. 15. Analysis of the behavior of the inverse correlation length κ for $R=\frac{1}{2}$ as $T\to 0$ K.

2. $R=\frac{1}{2}$

Since no phase transition occurs at a nonzero T_c for this ratio of interactions the short-range order "region" consists of all $T>0$. The variation of $T_c(R)$ for $R\to\frac{1}{2}$ suggests an exponential divergence of the correlation length. The spin-spin correlations $\Gamma(r)$ were therefore analyzed assuming a simple Ornstein-Zernike decay

$$\Gamma(r)=D\frac{\exp(-\kappa r)}{r^{1/2}} \quad . \tag{15}$$

The resultant estimates for κ are plotted in Fig. 15. The data are certainly consistent with an exponential decrease in κ (i.e., exponential increase in $\xi=\kappa^{-1}$) with $\bar{\nu}=1$

$$\kappa=\kappa_0\exp(-ct^{-1}) \quad . \tag{16}$$

The exponential singularity in ξ then suggests that

$$\chi^+T=\chi_0\exp(ct^{-\bar{\nu}}) \tag{17}$$

instead of the usual power-law divergence. (This is equivalent to $\nu=\infty$.) In Fig. 16 we show a semilog plot of χ^+T vs $t^{-\bar{\nu}}$ for several values of $\bar{\nu}$. The value

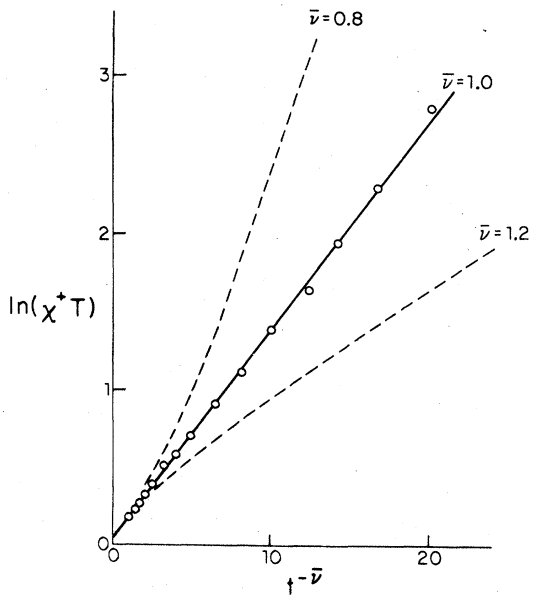

FIG. 16. Analysis of the behavior of the staggered susceptibility χ^+ for $R=\frac{1}{2}$ as $T\to 0$ K.

$\bar{\nu}=1$ clearly gives the best linear behavior over a wide range of temperature although values slightly different from $\bar{\nu}=1$ cannot be excluded.

C. Critical behavior

The behavior of the order parameter just below T_c was consistent with two-dimensional (2-D) Ising behavior with $\beta=\frac{1}{8}$ for all $R\neq\frac{1}{2}$. In Fig. 17 we show a log-log plot of m vs t. This plot shows that the asymptotic behavior does not appear until very small values of t when R is close to $\frac{1}{2}$. The critical amplitude also slowly increases as $R\rightarrow\frac{1}{2}$. It is, of course, possible that small deviations from a β value of $\frac{1}{8}$ do occur, particularly for $R>\frac{1}{2}$. The experimental uncertainty in the location of T_c limits our accuracy, and of course near $R=\frac{1}{2}$ crossover behavior between the $T=0, R=\frac{1}{2}$ transition and the asymptotic critical behavior associated with the R value being studied helps muddy the analysis.

The row spin-spin correlation functions were analyzed for $R<\frac{1}{2}$ and $T>T_c$ using an Ornstein-Zernike decay [Eq. (15)]. The resultant values for the inverse correlation length κ are shown in Fig. 18. These results also show that the asymptotic critical behavior for $R=0.45$ is not reached until very small values of t. The asymptotic behavior is consistent with a simple Ising model power-law divergence with $\nu=1$ for all R values. For $R=0.45$ and $t\gtrsim 0.4$ the temperature variation is consistent with the exponential decrease with temperature that was found for $R=\frac{1}{2}$ [see Eq. (16)]. This suggests that a substantial portion of the "critical region" is either dominated by the $T=0, R=\frac{1}{2}$ transition or is in the crossover region. The asymptotic critical behavior can then be seen only quite near to T_c.

The specific-heat data are not sufficiently precise or unrounded to enable us to fit the infinite lattice temperature dependence with a divergent form. We can, however, make use of finite-size scaling theory which

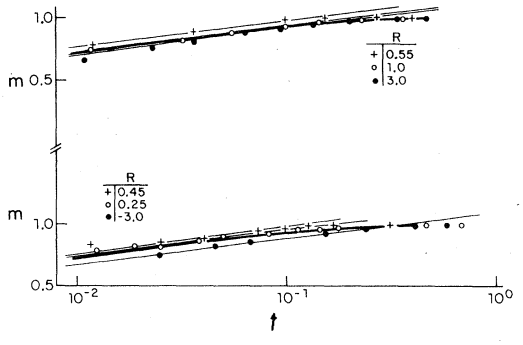

FIG. 17. Critical behavior of the order parameter m. The solid curves show the result for $R=0$.

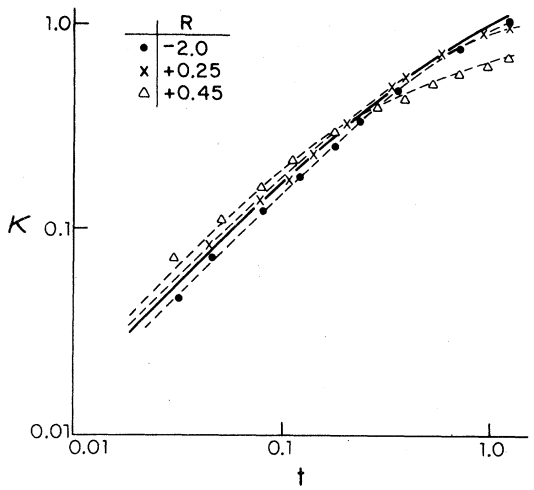

FIG. 18. Critical behavior of the inverse correlation length κ. The solid curve shows the behavior for $R=0$.

predicts that the size dependence of the maximum specific-heat value should vary as $L^{-\alpha/\nu}$. Semilog plots of the specific-heat maxima are shown in Fig. 19. For $R<\frac{1}{2}$ the data are consistent with the logarithmic behavior expected for $\alpha=0$ but with varying amplitude. The same is true for $R=+3.0$. For $R=+0.55$ the data appear to be increasing faster than $\ln L$ (i.e., indicating $\alpha/\nu>0$) but we cannot ex-

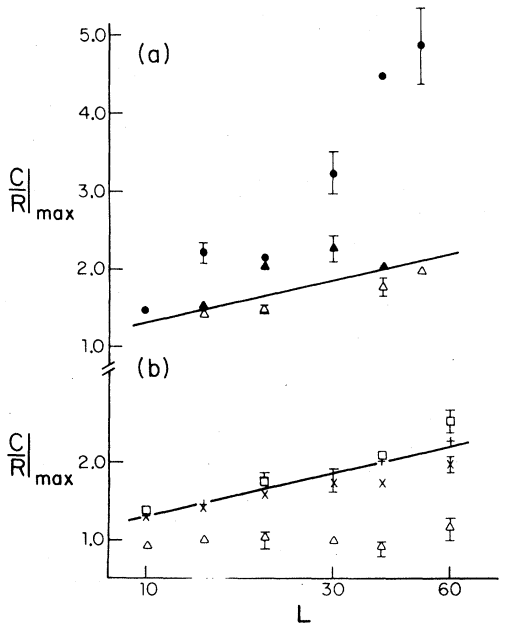

FIG. 19. Finite-size analysis of the specific-heat maximum C_{max}. (a) $R>\frac{1}{2}$: $R=0.55$, ●; $R=1.0$, ▲; and $R=3.0$, △. (b) $R<\frac{1}{2}$: $R=0.45$, △; $R=0.25$, ×; and $R=-3.0$, □. The straight lines show the $R=0$ behavior.

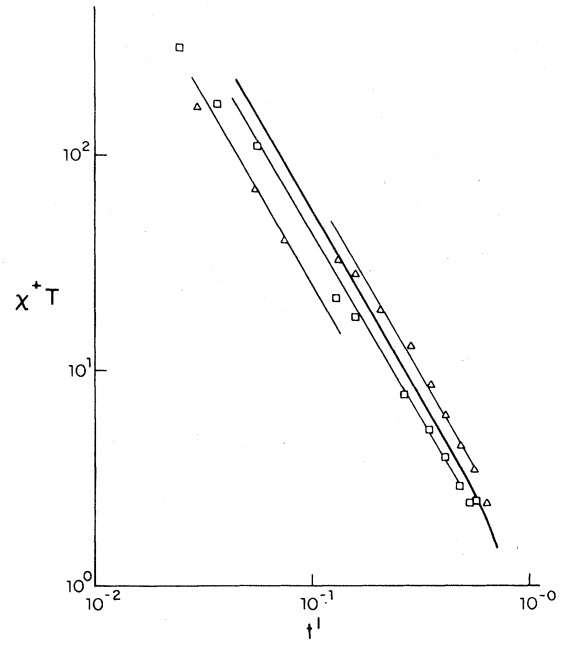

FIG. 20. Critical behavior of the staggered susceptibility. The solid curve shows the result for $R=0$. Data are for $R=-2.0$, □; and $R=+0.45$, Δ. ($t'=|1-T_c/T|$.)

clude the possibility that the variation is logarithmic but with a drastically altered amplitude.

The staggered susceptibility divergence is studied in Fig. 20 for several values of R. These data for $R=+0.45$ are difficult to interpret unambiguously. Either fluctuations or rounding dominate near T_c or the data show crossover from an exponential dependence at high temperature to a power law near T_c. Again Ising exponents with variable amplitudes can describe the results in general. The overall analysis of the critical behavior for r values near $\frac{1}{2}$ may well

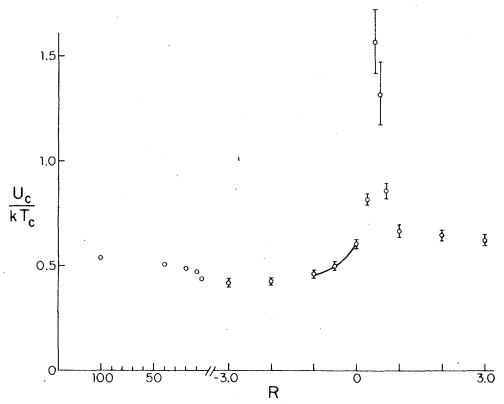

FIG. 21. Dependence of the critical internal energy U_c on R. The solid line shows the series-expansion result (see Ref. 15).

be complicated by crossover effects associated with the point $R=\frac{1}{2}, T_c=0$. This could be particularly bothersome for $R>\frac{1}{2}$ where any change in the critical exponents could be masked by crossover effects. For example, if ν decreases from the Ising value $\nu=1$ as R is lowered from $+\infty$, crossover to the point $R=\frac{1}{2}, T_c=0$ (which has $\nu=\infty$) could produce an effective $\nu_{\text{eff}}\approx 1$, thus obscuring any change from the Ising value. More detailed Monte Carlo calculations are underway for several values of $R>\frac{1}{2}$, including a magnetic field, and we hope the data will fully clarify the situation. The results of this study will be discussed elsewhere.[37]

The behavior of several nondivergent bulk quantities may also be analyzed at T_c. The critical internal energy at T_c is shown in Fig. 21. Over the range of R studied here there are variations by a factor of 4 in this quantity. Table I shows corresponding values for other nn models[9] for comparison. Similarly the criti-

TABLE I. Critical parameters for simple two- and three-dimensional lattices.[a]

Lattice	Honeycomb	square	triangle	diamond	sc	bcc	fcc	$S=\frac{1}{2}$ fcc Heisenberg
q[b]	3	3	6	4	6	8	12	12
U_c/kT_c	0.760	0.623	0.549	0.320	0.218	0.170	0.150	0.439
$(S_\infty-S_c)/k$	0.428	0.387	0.363	0.182	0.133	0.107	0.102	0.220
$kT\chi_c$	0.121	0.157	· · ·		0.340		0.369	
$qK_{\text{nn}}\chi_c$	0.240	0.277			0.452		0.465	
$qK_{nn}\chi_{\max}$	0.416	0.430	· · ·		0.464		0.473	
D		0.703	0.669		0.320	0.26	0.25	
B	1.265	1.222	1.203	1.661	1.570	1.491	1.488	

[a]Values in this table were obtained from Ref. 9.
[b]Coordination number for nn coupling only.

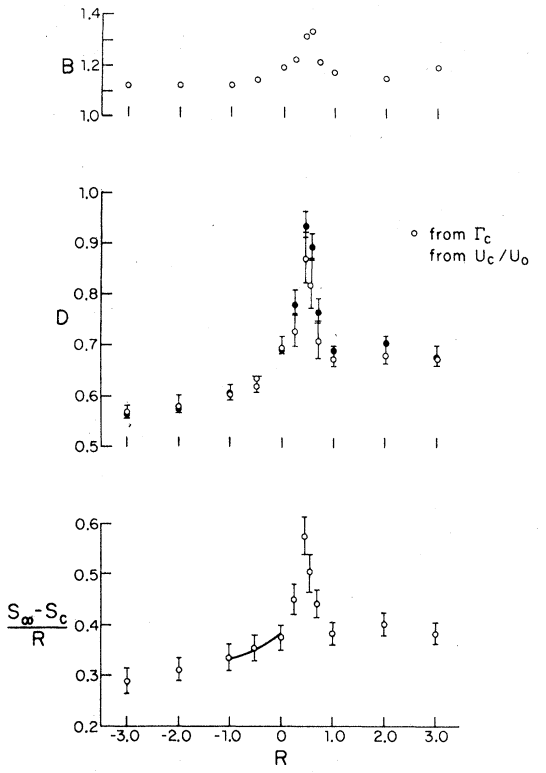

FIG. 22. Dependence of critical parameters on R. The solid line shows the series-expansion result (see Ref. 15).

cal entropy S_c was determined by numerical integration of C/RT and is shown as a function of R in Fig. 22. Since only data near T_c were obtained for $R < -3.0$, it was not possible to determine S_c for these R values. The variations of the critical internal energy and critical entropy are rather striking. Such variations have usually been ascribed to the effects of anisotropy (e.g., Ising versus Heisenberg model) or change in lattice dimensionality (see Table I). The spin-spin correlations were also analyzed at T_c assuming a simple critical behavior

$$\Gamma(r) = Dr^{-\eta} \ , \tag{18}$$

where $\eta = \frac{1}{4}$ for $R = 0$. Within experimental error we find $\eta = \frac{1}{4}$ for all R values and the resultant variation in D with R is plotted in Fig. 22. It has already been shown[9] that $D \approx U_c/U_0$ for the nearest-neighbor square and simple cubic lattices, so it would seem interesting to determine whether or not this remains valid for $R \neq 0$. The comparison in Fig. 22 suggests systematic differences although the two sets of points are within experimental error of each other. The order parameter critical amplitude is also plotted in Fig. 22 and also shows R dependence. These results show quite clearly the danger in deducing the effective dimensionality or interacting by merely "matching-up" values of critical parameters with specific model results.

V. CONCLUSION

We have determined the behavior of the thermal and magnetic properties of the Ising square lattice over a wide range of R (i.e., competing nn and nnn interactions). The results show a substantial variation in a number of characteristic critical "parameters" and amplitudes. No suggestion of non-Ising critical exponents is found for $R < \frac{1}{2}$. The special point $R = \frac{1}{2}, T_c = 0$, however, has an exponential divergence of the correlation length and susceptibility (i.e., ν and $\gamma = \infty$) and it is quite likely that crossover effects to this point complicate the analysis of the asymptotic critical behavior on the nearby phase boundaries. Although no conclusive evidence of non-Ising critical behavior is available for $R > \frac{1}{2}$, the analyses of the phase boundary crossover as $R \to \infty$ and $R \to \frac{1}{2}$ from above and of the size dependence of the specific-heat maximum suggest that nonuniversal behavior does appear. Much more detailed data will be needed, however, to definitively resolve this question.

ACKNOWLEDGMENTS

This research was supported in part by the NSF. We wish to thank Professor K. Binder and Dr. P. A. Lindgård for helpful discussions and suggestions.

[1]For a full review of the extensive work done on this model see B. M. McCoy and T. T. Wu, *The Two Dimensional Ising Model* (Harvard University, Cambridge, Mass., 1973).
[2]D. P. Landau, Phys. Rev. B 13, 2997 (1976).
[3]See, e.g., articles by L. P. Kadanoff and R. B. Griffiths, in *Critical Phenomena*, edited by M. S. Green (Academic, New York, 1971).
[4]K. Jüngling and G. Obermair, J. Phys. C 7, L363 (1974).
[5]K. Jüngling, J. Phys. C 8, L169 (1975).
[6]K. Jüngling, J. Phys. C 9, L1 (1976).
[7]L. J. de Jongh and A. R. Miedema, Adv. Phys. 23, 1 (1974).
[8]Adsorbed monolayers at 50% coverage are also good physical analogs of the nnn Ising square lattice. Monolayers of manganese stearate have been made and studied by Pomerantz, e.g., M. Pomerantz, Bull. Am. Phys. Soc. 22, 388 (1977).
[9]See, e.g., M. E. Fisher, Rep. Prog. Phys. 30, 615 (1967).

[10]W. Bitterlich and R. J. Jellito, Phys. Status Solidi 28, 365 (1968).
[11]A. E. Ferdinand and M. E. Fisher, Phys. Rev. 185, 832 (1969).
[12]A. Kawakami and T. Osawa, J. Phys. Soc. Jpn. Suppl. 26, 105 (1969).
[13]R. W. Gibberd, J. Math. Phys. 10, 1026 (1969).
[14]C. Fan and F. Y. Wu, Phys. Rev. 179, 560 (1969).
[15]N. W. Dalton and D. W. Wood, J. Math. Phys. 10, 1271 (1969).
[16]S. Takase, J. Phys. Soc. Jpn. 42, 1819 (1977).
[17]F. W. Wu, Phys. Rev. B 4, 2312 (1971).
[18]M. Nauenberg and B. Nienhius, Phys. Rev. Lett. 33, 944 (1974).
[19]J. M. J. van Leeuwen, Phys. Rev. Lett. 34, 1056 (1975).
[20]M. E. Fisher and W. J. Camp, Phys. Rev. Lett. 26, 565 (1971).
[21]M. P. Nightingale, Phys. Lett. A 59, 486 (1977).
[22]S. Krinsky and D. Mukamel, Phys. Rev. B 16, 2313 (1977); and E. Domany, M. Schick, J. S. Walker, and R. B. Griffiths, Phys. Rev. B 18, 2209 (1978).
[23]D. P. Landau, J. Appl. Phys. 42, 1284 (1971).
[24]S. Takase, J. Phys. Soc. Jpn. 40, 1240 (1976).
[25]See Refs. 26–28 and the extensive references contained therein.
[26]K. Binder, Adv. Phys. 23, 917 (1974).
[27]K. Binder, in *Phase Transitions and Critical Phenomena,* edited by C. Domb and M. S. Green (Academic, New York, 1976), Vol. 56.
[28]D. P. Landau, in *Proceedings of the 19th Conference on Mangetism and Magnetic Materials, Boston, 1973,* edited by C. D. Graham, Jr., and J. J. Rhyne, AIP Conf. Proc. No. 18 (AIP, New York, 1974), p. 819.
[29]M. E. Fisher, in *Proceedings of the International Summer School Enrico Fermi, Course 51, Varenna, Italy, 1970,* (Academic, New York, 1971).
[30]D. P. Landau, Phys. Rev. B 14, 255 (1976).
[31]T. S. Chang, L. L. Liu, D. N. Lambeth, and H. E. Stanley, Phys. Rev. B 11, 1254 (1975).
[32]E. K. Riedel and F. J. Wegner, Z. Phys. 225, 195 (1969).
[33]See, for example, S. Singh and D. Jasnow, Phys. Rev. B 11, 3445 (1975); M. E. Fisher and P. Pfeuty, *ibid.* 6, 1889 (1972); F. J. Wegner, *ibid.* 6, 1891 (1972).
[34]I. G. Enting, J. Phys. C 7, 1237 (1974).
[35]K. Binder and D. P. Landau, Phys. Rev. B 13, 1140 (1976).
[36]J. Stephenson, Phys. Rev. B 1, 4405 (1970); J. Stephenson and D. D. Betts, Phys. Rev. B 2, 2702 (1970).
[37]K. Binder and D. P. Landau, Phys. Rev. B (to be published).